ANL/CSE-14/9

Design of the Phase-2 Target for Mini-SHINE/MIPS Experiments

Chemical Science and Engineering Division

About Argonne National Laboratory
Argonne is a U.S. Department of Energy laboratory managed by UChicago Argonne, LLC under contract DE-AC02-06CH11357. The Laboratory's main facility is outside Chicago, at 9700 South Cass Avenue, Argonne, Illinois 60439. For information about Argonne and its pioneering science and technology programs, see www.anl.gov.

DOCUMENT AVAILABILITY

Online Access: U.S. Department of Energy (DOE) reports produced after 1991 and a growing number of pre-1991 documents are available free via DOE's SciTech Connect (http://www.osti.gov/scitech/)

Reports not in digital format may be purchased by the public from the National Technical Information Service (NTIS):
U.S. Department of Commerce
National Technical Information Service
5301 Shawnee Rd
Alexandra, VA 22312
www.ntis.gov
Phone: (800) 553-NTIS (6847) or (703) 605-6000
Fax: (703) 605-6900
Email: **orders@ntis.gov**

Reports not in digital format are available to DOE and DOE contractors from the Office of Scientific and Technical Information (OSTI):
U.S. Department of Energy
Office of Scientific and Technical Information
P.O. Box 62
Oak Ridge, TN 37831-0062
www.osti.gov
Phone: (865) 576-8401
Fax: (865) 576-5728
Email: **reports@osti.gov**

Disclaimer
This report was prepared as an account of work sponsored by an agency of the United States Government. Neither the United States Government nor any agency thereof, nor UChicago Argonne, LLC, nor any of their employees or officers, makes any warranty, express or implied, or assumes any legal liability or responsibility for the accuracy, completeness, or usefulness of any information, apparatus, product, or process disclosed, or represents that its use would not infringe privately owned rights. Reference herein to any specific commercial product, process, or service by trade name, trademark, manufacturer, or otherwise, does not necessarily constitute or imply its endorsement, recommendation, or favoring by the United States Government or any agency thereof. The views and opinions of document authors expressed herein do not necessarily state or reflect those of the United States Government or any agency thereof, Argonne National Laboratory, or UChicago Argonne, LLC.

ANL/CSE-14/9

Design of the Phase-2 Target for Mini-SHINE/MIPS Experiments

by
S. Chemerisov, J. Bailey, V. Makarashvili, B. Micklich, and G.F. Vandegrift
Chemical Science and Engineering Division, Argonne National Laboratory

prepared for
U.S. Department of Energy, National Nuclear Security Administration,
Office of Defense Nuclear Nonproliferation

July 31, 2012

CONTENTS

1 INTRODUCTION 1

1.1 Mini-SHINE/MIPS Experiments 2

2 TARGET DESIGNS 3

3 FINALIZED DESIGN 6

4 PHASE 2 MINI SHINE/MIPS DESIGN 10

5 CONCLUSION 13

APPENDIX A: DU Target Cooling Analysis for the Disk Target Design 15

FIGURES

1 Power Density and Neutron Flux in the Solid DUT Bombarded with a Beam of Electrons at 40-MeV Energy 4

2 Composite Target Design Utilizing Ta Center Piece to Tolerate High Energy in the Front Center of the Target and Results of the MCNPX Calculations of the Power Deposition for This Target Design 4

3 Power Deposition for Ta/DU Composite Target with Conical Cut in the Central Part of the Ta Center 5

4 Fraction of the Photo-neutrons Produced on Ta and DU Parts of the Target for Cylindrical and Conical Geometries 5

5 Energy Deposition in the Depleted Uranium Photo-neutron Converter, for the Irradiation Conditions Given in the Text 7

6 Parametric Plot of Heat Generation vs. Target Half Thickness for Disk Target Geometry 7

7 Fraction of the Photo-neutron Yield for Disk Target When All Disks are DU; Three Front Disks are Ta, and the Rest Are DU; and Five Front Disks are Ta, and the Rest Are DU 8

8 Side View of MCNPX Model Used for DU Target and Uranyl Nitrate Solution Calculations, and Top View of the MCNPX Model through the Beamline 10

FIGURES (Cont.)

9 MCNPX Model of the Target and Solution used in the Calculations..... 11

10 Fission Rates in the Uranyl Nitrate Solution, for the Irradiation Conditions Given in the Text 11

11 Energy Deposition in the Uranyl Nitrate Solution, for the Irradiation Conditions Given in the Text..... 12

TABLES

1 Fission and Energy Deposition Rate in the Depleted Uranium Target Disks..... 8

2 Summary of Photo-neutron Generation in Different Target Designs; Neutron Yield is Calculated in Number of Neutrons per Source Electron..... 9

DESIGN OF THE PHASE-2 TARGET FOR MINI-SHINE/MIPS EXPERIMENTS

1 INTRODUCTION

Under the National Nuclear Security Administration's Global Threat Reduction Initiative (GTRI), Argonne National Laboratory (Argonne) is assisting three potential domestic producers to develop and implement molybdenum-99 (Mo-99) production in the United States without the use of highly enriched uranium (HEU). Two of the potential domestic producers are Babcock and Wilcox Technical Services Group (B&W) and Morgridge Institute for Research (MIR).

B&W is developing the Medical Isotope Production System (MIPS). In this system, the Mo-99 is produced in an LEU-fueled Aqueous Homogenous Reactor (AHR) by the fissioning of uranium-235 (U-235). The MIPS consists of an AHR containing a low enriched uranium (LEU) solution, a molybdenum-extraction system utilizing a chromatographic column, and a reactor off-gas and solution-control systems. The use of AHRs presents an attractive alternative to the conventional target-irradiation method for producing Mo-99 because the fuel solution itself is used to produce Mo-99, eliminating the need for targets. AHRs also operate at a much lower power level than that required for a traditional reactor. The three areas of Argonne research and development (R&D) are (1) radiolytic-gas generation in the fuel solution, (2) effects of fission and radiation on reactor-solution chemistry, and (3) development and optimization recovery of molybdenum from the irradiated fuel solution.

The first solution reactors earned the name "water-boilers" because of the observed bubbling or foaming that results from the radiolytic decomposition of water by fission fragments and subsequent evolution of radiolytic gases (hydrogen and oxygen). Because the nitrate ion also undergoes radiolytic decomposition, uranyl-nitrate-based AHRs will also generate nitrogen compounds from the nitrite ion to ammonia (N^{3+} to $^{3-}$), NO_2^-, N_2, NO_x, and NH_3. Nitrogen, nitrogen oxides, and ammonia could potentially all be observed in the off-gas. The radiolytic decomposition of nitrate ions will also have the effect of increasing the pH of the fuel solution. The rate and composition of the radiolytic gas generation is of practical importance for the design and operation of AHR for two reasons. First, the design of the reactor off-gas system depends on the generation rate and the composition of the gas stream. Second, an increase of the fuel-solution pH can lead to the formation of metal-hydroxide precipitates and, therefore, must be controlled.

While the radiation chemistry of nitrate solutions has been investigated over the past 50 years, not much attention was given to the analysis of gas evolution, especially at high radiation doses. Observations of the formation of nitrogen-containing gases under radiation are numerous, but N_2, NO_x, and NH_3 formation have not been studied systematically; no mechanism for the formation of those gases was proposed. In addition, the reported values of the radiolytic yields for these gases from different sources vary by an order of magnitude. The goal of the off-gas measurement system of the mini-SHINE/MIPS experiments is to obtain reliable data for radiolytic gas generation in solutions that are of practical interest to the MIPS.

MIR and its partners are currently developing the SHINE system, which creates Mo-99 by neutron-induced fission of LEU in a subcritical aqueous solution. SHINE will produce primary neutrons by the collision of a beam of deuterium (D) ions with a tritium (T) gas target; these high-energy neutrons will induce fission in the U-235 in solution. Fission-produced Mo-99 can be extracted from the aqueous solution and purified. Argonne tasks for SHINE development parallel those for the MIPS development; we are developing an understanding of the solution chemistry under operating conditions and developing the Mo-recovery and purification system.

1.1 MINI-SHINE/MIPS EXPERIMENTS

The mini-SHINE/MIPS experiments will be performed using the high-current electron linac at Argonne's Low Energy Accelerator Facility (LEAF). The experiments will use an electron/x-ray/neutron convertor to produce neutrons that will produce fission in solution. The solution will be a 90- to 150-g-U/L LEU uranyl nitrate or uranyl-sulfate solution. In phase 1, the convertor is tantalum, and the target solution has a volume of 5 L; this configuration will generate a peak fission power density of up to 0.1 W/mL.

In phase 2, the convertor will be depleted uranium (DU), beam power will increase 20 kW, and the solution volume will be 20 L; this configuration will generate a peak fission power density of up to 1 W/mL. The volumes of the actual MIPS and SHINE units will be much larger, however: 200 to 500 L. The purpose of this report is to describe the current design of the phase 2 target and irradiation volume, and to analyze expected neutron and thermo-hydraulic performance of the system.

2 TARGET DESIGNS

Several target design configurations were evaluated for photo-neutron and thermal-hydraulic performance. For each configuration, heat generation within the target was obtained from the MCNPX (Monte Carlo N-Particle eXtended) particle transport code. A 20-kW beam power was assumed for all the cases. In general, it should be noted that the heat generation profile is Gaussian radially and is peaked very near the front of the target (Figure 1). As a result, this profile has a significant and rather problematic impact on the thermal hydraulic design. Material properties were assumed constant at an average operating temperature. The convective boundary conditions at the surface of the target were determined using "Dittus-Bolter" correlations.

As a first target concept, a simple solid cylinder of DU target material with ambient temperature water flow at the cylinder's sides was considered. Approximate hand calculations clearly indicated that the temperature at the axial centerline near the front face would be extremely high and well above the assumed maximum allowable operating temperature of the DU. A 300°C maximum operating temperature for the DU was chosen to avoid grain growth in the DU.

A second target concept was developed based on the results from the first analysis. The extremely high temperature at the center of the DU target was clearly due to the thermal resistance of the DU in the radial direction. This second concept incorporated high thermal conducting aluminum disks placed between thin DU disks in order to reduce the radial thermal resistance. Based on a calculation for a one-dimensional radial model, it was apparent that the thermal conductance in the aluminum disks was not high enough to lower the centerline temperature of the target to an acceptable level.

Because energy deposition is so front peaked, a third target concept was developed that incorporated a compound configuration of the target with Ta cylinder at the center front of the target, where the heat generation is high, surrounded by DU. The Ta material has a very high melting point; hence, this design removes the 300°C centerline-temperature limitation for the front center of the target. The configuration of this target is shown in Figure 2. The smaller (1.5-cm diameter by 2.5 cm) Ta cylinder is located at the front where the electron beam impinges the target. There are 0.2-cm gaps around the Ta target for coolant flow, as well as a 0.5-cm gap at the back. There are two flow divider bars, located 180 degrees apart, that run the length of the Ta. Flow is assumed to enter at one side of the dividers and then be returned via the back gap and go out the other side of the dividers. Flow in these channels is assumed to be 12 m/s ambient-temperature water. A similar flow channel configuration is located around the outside of the DU cylinder. Calculations were performed to determine the surface temperature of the Ta. The heat flux at the Ta target surface (Ta/water interface) was assumed to be uniform with a total heat loss from the Ta target of 69% of the beam power (obtained from MCNPX computer code). This calculation indicated that, at a minimum, the surface temperature was 167°C. Therefore, in order to prevent boiling in the channel (a preferred condition), the operating pressure of the coolant system had to be at a minimum 6.8 atm (100 psig).

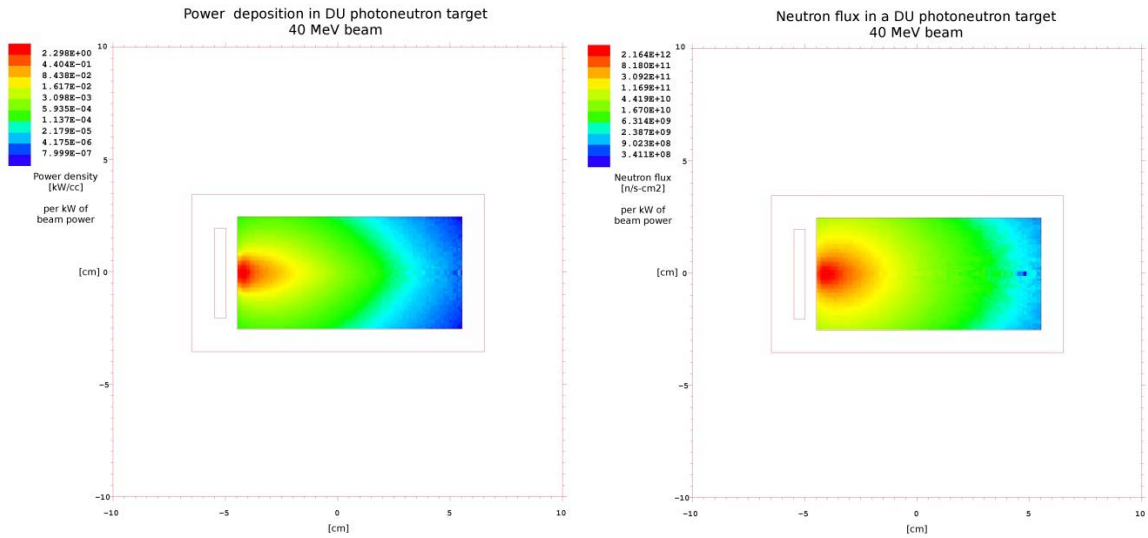

FIGURE 1 Power Density and Neutron Flux in the Solid DUT Bombarded with a Beam of Electrons at 40-MeV Energy (Energy is deposited in very narrow region of the target, while neutron flux is spread out through the larger volume.)

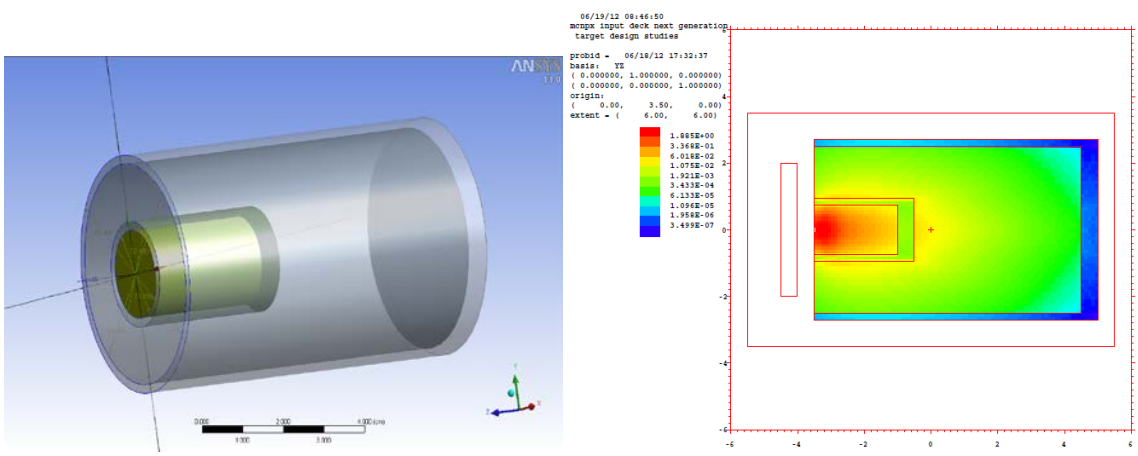

FIGURE 2 Composite Target Design Utilizing Ta Center Piece to Tolerate High Energy in the Front Center of the Target (left) and Results of the MCNPX Calculations of the Power Deposition for This Target Design (right)

In order to distribute the heat more uniformly within the Ta, a cone-shaped cutout in the front of the Ta target was considered (Figure 3). MCNPX simulations of the neutron fluxes for the composite targets design revealed that composite target is only marginally superior to the solid Ta target (neutron flux increase is only 15%), which cannot justify the complexity of the target utilizing DU. In general, the thermal hydraulic performance of the DU portion of the target assembly did not pose any significant problems. Figure 4 represents results of the MCNPX calculations of the photo-neutron fractions produced in Ta and DU parts of the composite targets.

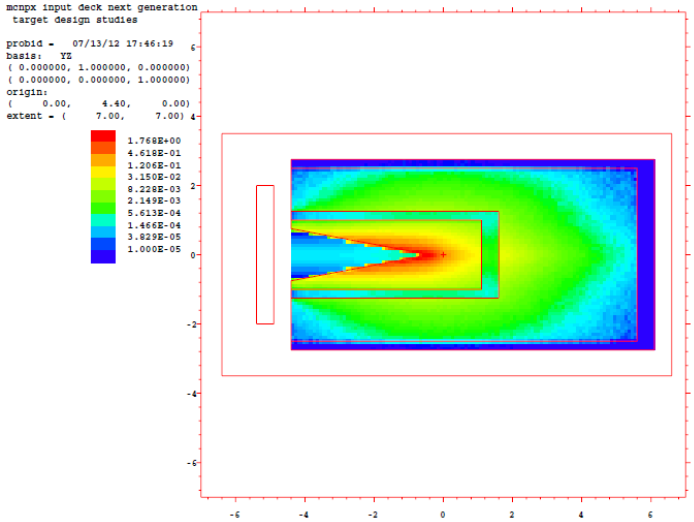

FIGURE 3 Power Deposition for Ta/DU Composite Target with Conical Cut in the Central Part of the Ta Center (Power distribution in the target is spread out more, allowing cooling with water at ambient pressure.)

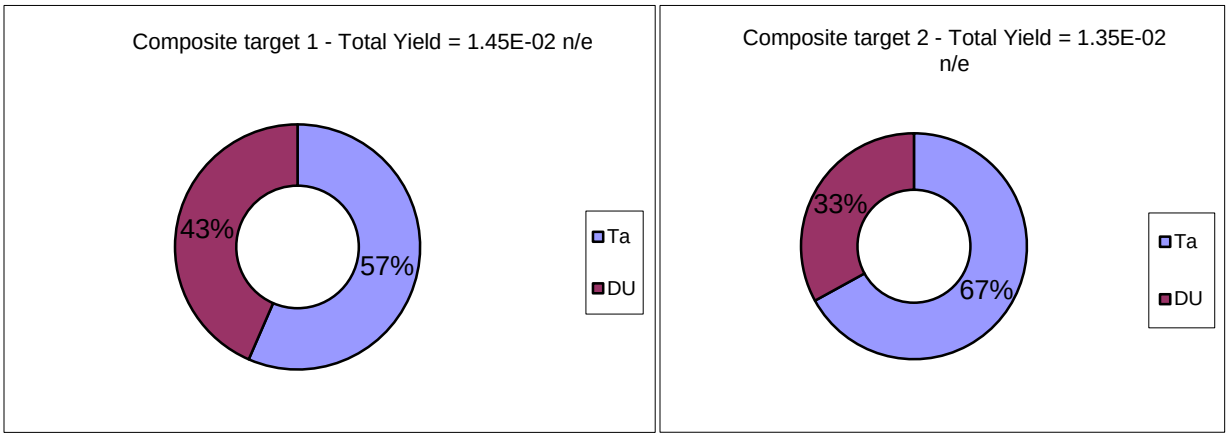

FIGURE 4 Fraction of the Photo-neutrons Produced on Ta and DU Parts of the Target for Cylindrical (left) and Conical (right) Geometries (Only a small fraction of the neutrons is produced in DU part of the target.)

3 FINALIZED DESIGN

Previous MCNPX simulations suggested a neutron flux from the solid DU target that was twice as high as that of the solid Ta target, so to use this advantage, the target must consist of mostly DU. The only configuration that has a chance of improved heat dissipation would be a target consisting of thin disks separated by narrow water channels. A layout of this concept is shown in Figure 5. In this concept, all disks have a diameter of 50 mm; disks 1–10 are 2 mm (1.5 mm DU and 0.05 mm Zr), and disks 11–22 are 6 mm thick (5 mm DU and 1 mm Zr). One-dimensional calculations modeling the worst-case disk location were performed. First, a parametric plot of disk thickness versus heat generation was developed using the one-dimensional heat conduction model, as shown in Figure 6. Two design criteria are shown on this plot. The disk center-temperature curve is determined by the 300°C allowable DU temperature. The second curve is determined by maintaining the surface temperature of the disk below 100°C in order to avoid boiling in the channel. As indicated by this plot, the center temperature of the disk is the criterion that limits the disk thickness except for very thin disks. Based on the results from the neutronics calculations, the maximum heat-generation rate is 4.6 kW/cm^3. Using this value, the parametric plot indicates that the maximum disk thickness at the worst case location is 0.35 cm (3.5 mm). Further, it was determined from the one-dimensional analysis that at approximately 3 cm from the front of the target the disk thickness could be increased to 1 cm without exceeding the center temperature criteria. In addition, a one-dimensional hydraulic model calculation was performed that indicated that at 12-m/s flow speed the pressure drop across the disk channel was approximately 1 atm. The detailed analysis of thermo-hydraulic performance of the target is given in Appendix A.

Figure 5 shows the energy deposition inside the target in W/cm^3/kW$_{beam}$. The Continuous Slowing Down Approximation CSDA range of a 35-MeV electron in uranium is 12.35 g/cm^2. At a mass density of 19.3 g/cm^3, this means that the maximum penetration of the source electrons into the uranium converter is about 0.644 cm (neglecting any slowing in the Zircaloy cladding or the water coolant), or near the front of the fourth DU disk. Because disks 11–22 are three times thicker than disks 1–10, energy deposition per disk rises from disk 10 to 11 (see Table 1). Table 1 shows the results for neutron- and photon-induced fission rates and the energy deposited in each disk in watts/kWbeam. All results have been normalized to 1 kW of electron beam power. The energy deposition figures for the disks include that deposited inside the cladding.

We have also considered replacing several of the front disks with the highest energy deposition density with Ta to increase power envelope of the target. A summary of the results of the MCNPX calculations for those three cases are presented in Figure 7. The main conclusion from those calculations is that replacement of DU disks for Ta leads to significant decrease of neutron flux, so to achieve a superior neutronics performance, the target must be constructed completely from DU.

In Table 2 results of the MNCPX calculations for different target designs are summarized. The best photo-neutron yield is achieved for target design composed of DU disks. Thermal calculation has also shown that we can cool the target if the size of the beam is kept above 1.8-cm full width at half maximum (FWHM).

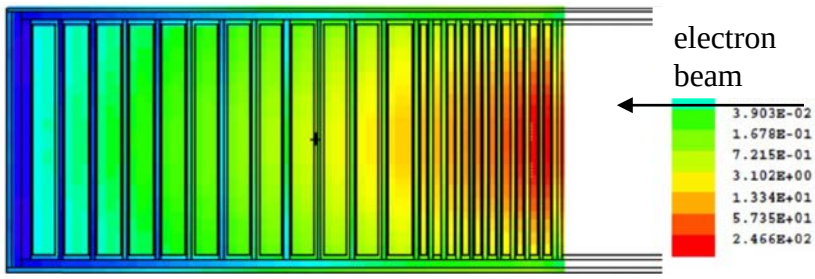

FIGURE 5 Energy Deposition ($W/cm^3/kW_{beam}$) in the Depleted Uranium Photo-neutron Converter, for the Irradiation Conditions Given in the Text

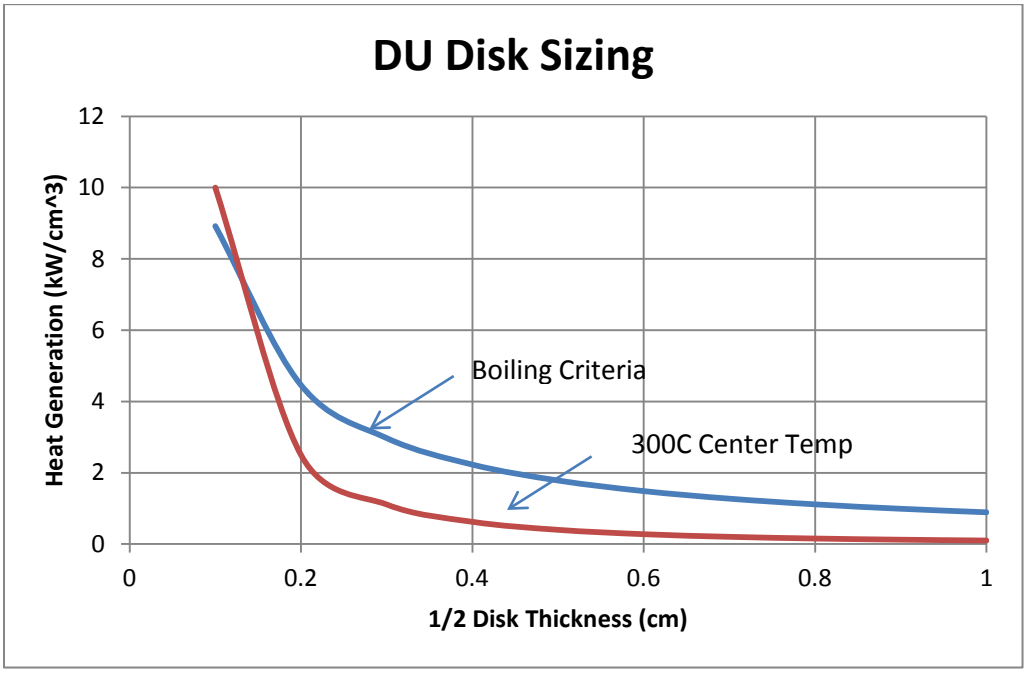

FIGURE 6 Parametric Plot of Heat Generation vs. Target Half Thickness for Disk Target Geometry (The red line is defined by 300°C maximum temperature in DU disk; the blue line is defined by 100°C maximum surface temperature to prevent boiling of the coolant.)

TABLE 1 Fission and Energy Deposition Rate in the Depleted Uranium Target Disks

Disk No.	Neutron-Induced Fissions/kW_{beam}	Photon-Induced Fissions/kW_{beam}	Energy Deposition W/kW_{beam}
1	4.03×10^{9}	3.26×10^{10}	1.83×10^{2}
2	4.76×10^{9}	5.93×10^{10}	2.03×10^{2}
3	4.90×10^{9}	5.49×10^{10}	1.20×10^{2}
4	4.73×10^{9}	4.37×10^{10}	6.32×10^{1}
5	4.44×10^{9}	3.47×10^{10}	4.36×10^{1}
6	4.14×10^{9}	2.77×10^{10}	3.46×10^{1}
7	3.81×10^{9}	2.23×10^{10}	2.81×10^{1}
8	3.51×10^{9}	1.79×10^{10}	2.30×10^{1}
9	3.24×10^{9}	1.44×10^{10}	1.88×10^{1}
10	3.00×10^{9}	1.16×10^{10}	1.54×10^{1}
11	8.89×10^{9}	2.55×10^{10}	3.49×10^{1}
12	7.37×10^{9}	1.34×10^{10}	1.97×10^{1}
13	6.25×10^{9}	7.03×10^{9}	1.13×10^{1}
14	5.44×10^{9}	3.72×10^{9}	6.48×10^{0}
15	4.87×10^{9}	1.98×10^{9}	3.79×10^{0}
16	4.44×10^{9}	1.06×10^{9}	2.24×10^{0}
17	4.06×10^{9}	5.66×10^{8}	1.36×10^{0}
18	3.81×10^{9}	3.04×10^{8}	8.46×10^{-1}
19	3.57×10^{9}	1.64×10^{8}	5.46×10^{-1}
20	3.43×10^{9}	8.95×10^{7}	3.70×10^{-1}
21	3.37×10^{9}	4.90×10^{7}	2.68×10^{-1}
22	3.37×10^{9}	2.72×10^{7}	2.12×10^{-1}
Total	9.94×10^{10}	3.73×10^{11}	8.14×10^{2}

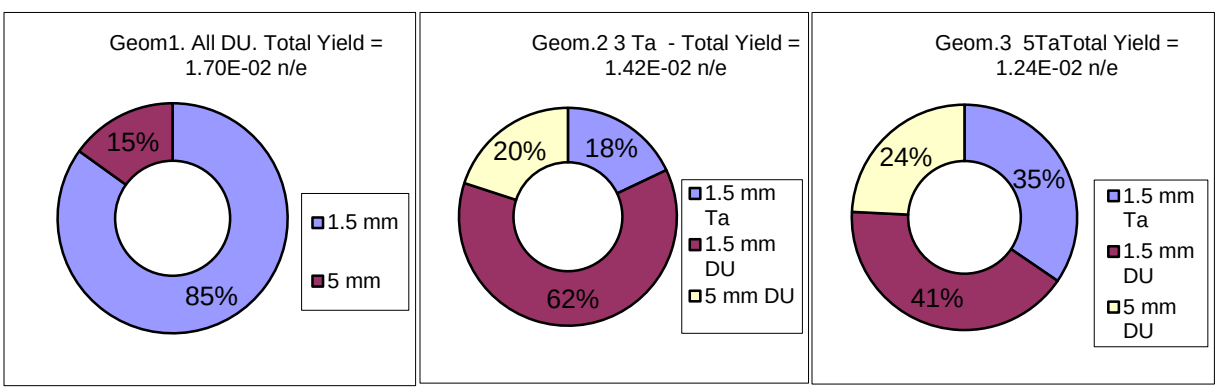

FIGURE 7 Fraction of the Photo-neutron Yield for Disk Target When All Disks are DU (left); Three Front Disks are Ta, and the Rest Are DU (center); and Five Front Disks are Ta, and the Rest Are DU (right) (The neutron yield drops significantly with introduction of Ta disks.)

TABLE 2 Summary of Photo-neutron Generation in Different Target Designs; Neutron Yield is Calculated in Number of Neutrons per Source Electron

	Composite Target: Cylinder		Composite Target: Conical		Disk Target: All DU		Disk Target: 3 Ta, Rest DU			Disk Target: 5 Ta, Rest DU		
Nuclear Process	Ta	DU	Ta	DU	1.5 mm	5 mm	1.5 mm Ta	1.5 mm DU	5 mm DU	1.5 mm Ta	1.5 mm DU	5 mm DU
Capture	-1.10×10^{-4}	-2.08×10^{-4}	-2.05×10^{-4}	-2.37×10^{-4}	-1.18×10^{-4}	-7.70×10^{-5}	-7.38×10^{-5}	-7.46×10^{-5}	-7.56×10^{-5}	-1.22×10^{-4}	-4.48×10^{-5}	-7.30×10^{-5}
(n,xn)	6.60×10^{-6}	3.35×10^{-5}	6.80×10^{-6}	2.38×10^{-5}	2.35×10^{-5}	1.22×10^{-5}	2.00×10^{-6}	1.29×10^{-5}	7.70×10^{-6}	4.50×10^{-6}	7.60×10^{-6}	1.31×10^{-5}
Loss to (n,xn)	-3.10×10^{-6}	-1.66×10^{-5}	-3.30×10^{-6}	-1.17×10^{-5}	-1.17×10^{-5}	-6.10×10^{-6}	-1.00×10^{-6}	-6.40×10^{-6}	-3.80×10^{-6}	-2.20×10^{-6}	-3.80×10^{-6}	-6.50×10^{-6}
Fission	0.00×10^{0}	6.08×10^{-4}	0.00×10^{0}	5.19×10^{-4}	4.17×10^{-4}	2.17×10^{-4}	0.00×10^{0}	2.55×10^{-4}	2.24×10^{-4}	0.00×10^{0}	1.44×10^{-4}	2.15×10^{-4}
Loss to Fission	0.00×10^{0}	-2.20×10^{-4}	0.00×10^{0}	-1.86×10^{-4}	-1.48×10^{-4}	-7.84×10^{-5}	0.00×10^{0}	-9.09×10^{-5}	-7.94×10^{-5}	0.00×10^{0}	-5.18×10^{-5}	-7.66×10^{-5}
Photonuclear	8.29×10^{-3}	3.15×10^{-3}	9.27×10^{-3}	2.24×10^{-3}	7.45×10^{-3}	1.30×10^{-3}	2.62×10^{-3}	4.55×10^{-3}	1.41×10^{-3}	4.41×10^{-3}	2.65×10^{-3}	1.51×10^{-3}
Photofission	0.00×10^{0}	2.95×10^{-3}	0.00×10^{0}	2.12×10^{-3}	6.84×10^{-3}	1.20×10^{-3}	0.00×10^{0}	4.17×10^{-3}	1.35×10^{-3}	0.00×10^{0}	2.42×10^{-3}	1.43×10^{-3}
Total	8.19×10^{-3}	6.30×10^{-3}	9.07×10^{-3}	4.47×10^{-3}	1.45×10^{-2}	2.57×10^{-3}	2.55×10^{-3}	8.81×10^{-3}	2.84×10^{-3}	4.29×10^{-3}	5.13×10^{-3}	3.01×10^{-3}
Total for the Target		1.45×10^{-2}		1.35×10^{-2}		1.70×10^{-2}			1.42×10^{-2}			1.24×10^{-2}

4 PHASE 2 MINI SHINE/MIPS DESIGN

We have conducted calculations for irradiation of 20 L of a 1-M uranyl-nitrate solution using 35-MeV electrons incident on a disk design of depleted uranium target. The target consists of ten disks of 1.5-mm-thick DU clad with 0.25-mm Zircaloy 4 on the faces and 0.5-mm Zircaloy 4 on the edges, followed by 12 disks of 5-mm-thick DU clad with 0.5-mm Zircaloy 4 on the faces and edges. The target disks are 5 cm in diameter and are separated by 1-mm water-filled cooling channels. There is a 1-mm-thick Inconel entrance window. The rest of the target is similar to that used with the tantalum photo-neutron converter in phase 1 experiments.

The incident electrons are modeled as a Gaussian beam with FWHM = 1.8 cm, three times the width of the beam used with the Ta target in phase 1. The geometry of the target and solution is shown in Figure 8, and a close-up view of the target is shown in Figure 9. The solution container is surrounded by a water reflector with a thickness of about 13 cm.

The transport calculations were performed using version 2.6.0 of the radiation transport code MCNPX. Tallies were made of the energy deposited and fission rate in each disk; the energy deposited in the remaining cells surrounding the target region; and the fission rate inside the uranyl nitrate solution.

Figures 10 and 11 show fission rates and energy deposition in the uranyl nitrate solution (because of the nature of these tallies, they have no meaning inside the part of the geometry covered by the target).

The total energy deposited in the uranyl nitrate solution is about 155 W/kW. For 20 kW of incident electron beam power, the average energy deposition will be about 0.15 W/cm^3. Figure 5 shows that the maximum energy deposition in the solution will be about 0.05W/cm^3/kW, or about 1.0 W/cm^3 for 20 kW of incident electron beam.

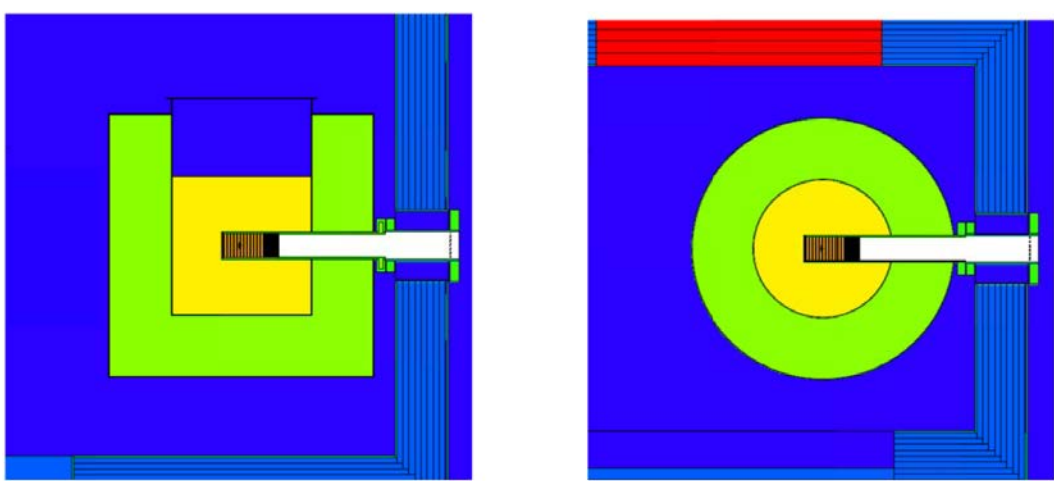

FIGURE 8 Side View of MCNPX Model Used for DU Target and Uranyl Nitrate Solution Calculations (left), and Top View of the MCNPX Model through the Beamline (right) (The beam is incident from the right in both images.)

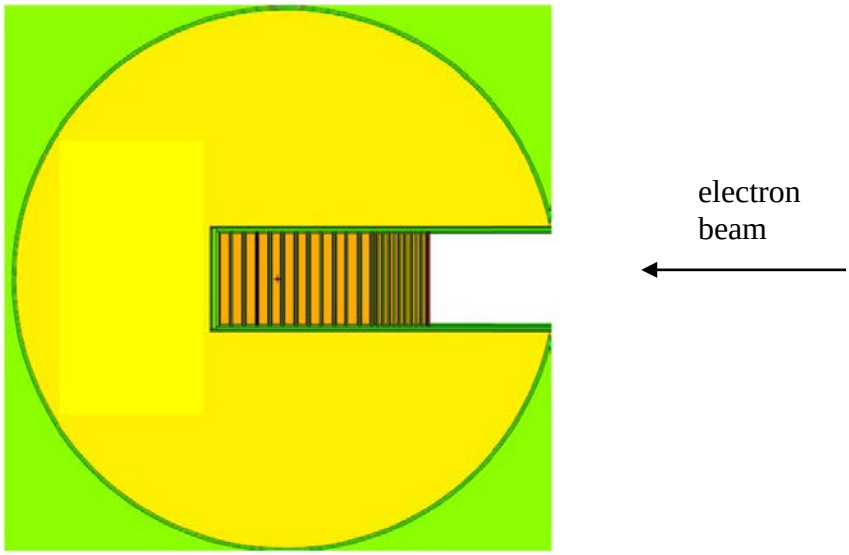

FIGURE 9 MCNPX Model of the Target and Solution used in the Calculations (The beam is incident from the right.)

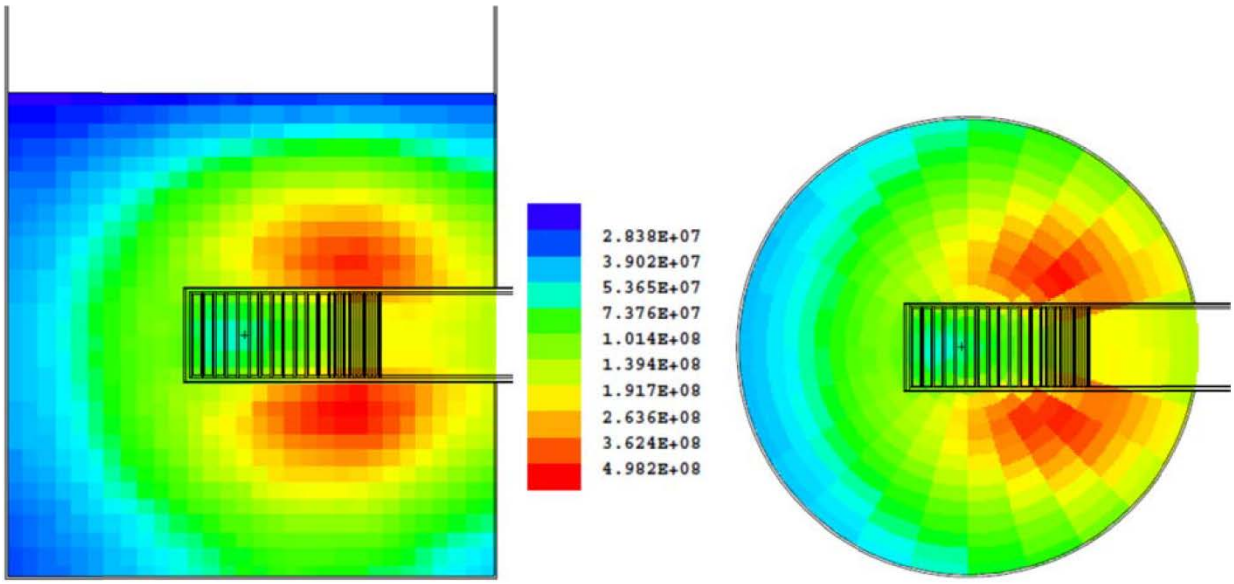

FIGURE 10 Fission Rates (fissions/cm^3/kW) in the Uranyl Nitrate Solution, for the Irradiation Conditions Given in the Text (left = side view; right = top view)

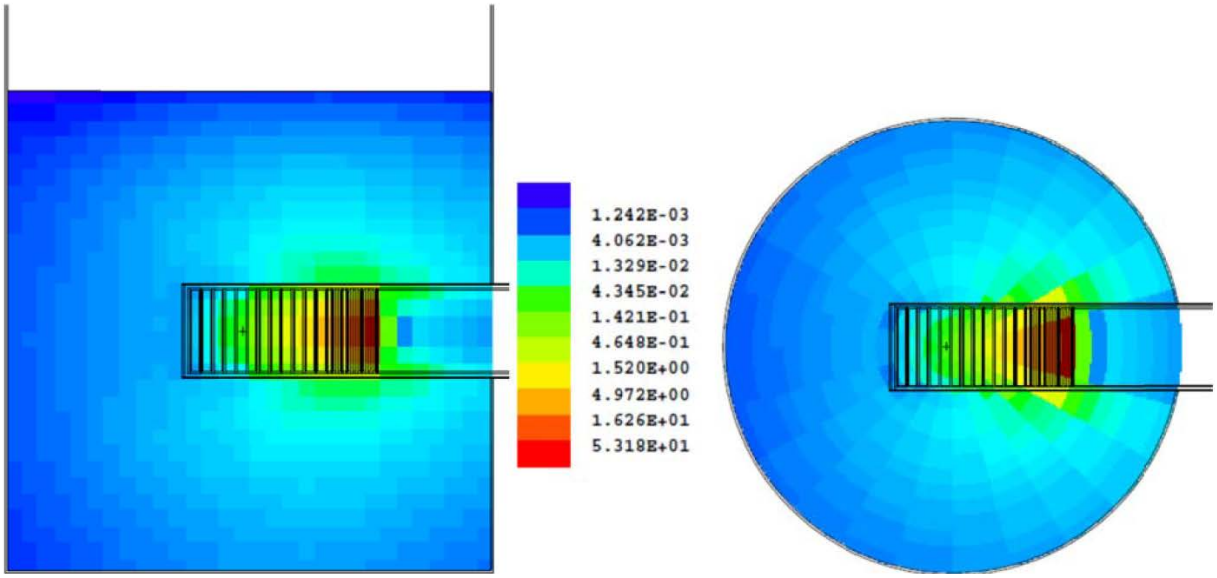

FIGURE 11 Energy Deposition (W/cm^3/kW) in the Uranyl Nitrate Solution, for the Irradiation Conditions Given in the Text (left = side view; right = top view)

5 CONCLUSION

Preliminary design of the photo-neutron target for phase 2 of the mini-SHINE/MIPS experiment is complete. The most promising design in terms of photo-neutron yield and thermo-hydraulic performance is the target consisting of DU disks separated by narrow cooling channels. MCNPX and thermo-hydraulic calculation for this target were performed and showed satisfactory performance of the target with projected operation parameters for the upgraded linac facility at Argonne. Using conservative estimations, the peak power in solution in the phase 2 mini-SHINE/MIPS experiment will reach 1 W/cm^3 with average power on the order of 0.15 W/cm^3. This new design will allow experimental studies of radiolysis of fissioning solutions of uranium salts and optimize the Mo-99 separation scheme under plant-relevant conditions.

This page intentionally left blank

APPENDIX A

DU TARGET COOLING ANALYSIS FOR THE DISK TARGET DESIGN

This page intentionally left blank

APPENDIX A:

DU TARGET COOLING ANALYSIS FOR THE DISK TARGET DESIGN

For calculations, the following properties for the cooling water were used:

$\rho_{h2o} := 62.3 \frac{lbm}{ft^3}$ Density

$Cp_{h2o} := 1 \frac{Btu}{lbm \cdot \Delta°F}$ Heat capacity

$\nu_{h2o} := 1 \cdot 10^{-5} \frac{ft^2}{s}$ Dynamic viscosity

$k_{h2o} := .347 \frac{Btu}{hr \cdot ft \cdot \Delta°F}$ Thermal conductivity

$Pr_{h2o} := 6.8$ Prandtl number

The channel geometry was assumed to be

$w_{chn} := 1mm$ Channel width

$D_{chn} := 2 \cdot w_{chn}$ Hydraulic diameter

The thermal convective coefficient in the flow channel between the disks is calculated first. The hydraulic diameter for this channel is approximated by assuming that the flow is between two infinite plates (i.e., 2 times channel width). The average water flow velocity in the channel is assigned a given value. From these values the Reynolds number is calculated. The Reynolds number is well above 10,000, therefore the flow is fully turbulent and the Nusselt number is determined using the correlation for turbulent flow. By definition of the Nusselt number, the thermal convective coefficient in the channel is calculated.

$v_{chn} := 40\frac{ft}{s}$ Average water flow velocity in channel

$Re_{chn} := \frac{v_{chn} \cdot D_{chn}}{\nu_{h2o}} = 2.625 \times 10^4$ Reynolds number > 10,000, turbulent flow

$Nu_{chn} := 0.023 \cdot Re_{chn}^{.8} \cdot Pr_{h2o}^{.33} = 148.496$ Nusselt number for turbulent flow

$h_{chn} := \frac{Nu_{chn} \cdot k_{h2o}}{D_{chn}} = 7.853 \times 10^3 \cdot \frac{Btu}{hr \cdot ft^2 \cdot \Delta°F}$ Thermal convective coefficient

$h_{chn} = 4.459 \times 10^{-3} \cdot \frac{kW}{cm^2 \cdot \Delta°C}$

Next, the heat flux into the flow channel is determined by assuming symmetry at the mid-plane of the disk. The peak heat generation is used to determine the total heat generated in the half volume of the disk. Note that the beam size here has been increased to three times the previous assumed size, which reduces the peak energy by one-ninth. The heat flux at the surface is then calculated assuming a uniform distribution. The difference between the surface and bulk temperature is then calculated from the convective heat transfer relation given in Kreith (1973)

$t_{disc} := .75mm$ distance to centerline of disk

$P_{beam} := 20kW$ Beam power

$q_{density} := \frac{1.89}{cm^3} \cdot P_{beam} \cdot \frac{1}{9} = 4.2 \cdot \frac{kW}{cm^3}$ Heat generation considering 3 X normal beam width

$q_{flux} := q_{density} \cdot t_{disc} = 0.315 \cdot \frac{kW}{cm^2}$ Heat flux into channel

$\Delta T_{SurBulk} := \frac{q_{flux}}{h_{chn}} = 70.642 \cdot \Delta°C$ Difference between bulk water temperature and disk surface temperature

Appendix A Reference

Kreith, F., 1973 , “Principles of Heat Transfer,” 7rd Edition, Intext Educational Publ.

Chemical Science and Engineering Division
Argonne National Laboratory
9700 South Cass Avenue, Bldg. 205
Argonne, IL 60439-4837

www.anl.gov

Argonne National Laboratory is a U.S. Department of Energy
laboratory managed by UChicago Argonne, LLC